MethodsX 6 (2019) 1999–2012

Contents lists available at ScienceDirect

MethodsX

journal homepage: www.elsevier.com/locate/mex

Method Article

Synthesis and characterization of Au nanoshells with a magnetic core and betaine derivatives

Tomas Bertok[a,b], Lenka Lorencova[a,b], Stefania Hroncekova[a], Veronika Gajdosova[a], Eduard Jane[a], Michal Hires[a], Peter Kasak[c,**], Ondrej Kaman[d], Roman Sokol[e], Vladimir Bella[f], Anita Andicsova Eckstein[g], Jaroslav Mosnacek[g], Alica Vikartovska[a], Jan Tkac[a,b,*]

[a] Institute of Chemistry, Slovak Academy of Sciences, Dubravska cesta 9, Bratislava 845 38, Slovak Republic
[b] Glycanostics Ltd., Dubravska cesta 9, Bratislava 845 38, Slovak Republic
[c] Center for Advanced Materials, Qatar University, P.O. Box 2713, Doha, Qatar
[d] Institute of Physics of the Czech Academy of Sciences, Cukrovarnicka 10/112, Prague 162 00, Czech Republic
[e] Private Urological Ambulance, Piaristicka 6, Trencin 911 01, Slovak Republic
[f] St. Elisabeth Cancer Institute, Heydukova 10, Bratislava 812 50, Slovak Republic
[g] Polymer Institute, Slovak Academy of Sciences, Dubravska cesta 9, Bratislava 845 41, Slovak Republic

A B S T R A C T

The article describes preparation, characterization and further modification of hybrid magnetic particles (Au nanoshells with a magnetic core (MPs@silica@Au)) by zwitterionic molecules bearing diazonium functional groups. Such hybrid magnetic particles modified by zwitterionic molecules exhibit the following features:

- Responsiveness towards external magnetic field applicable for various enrichment strategies due to magnetic core;
- Golden outer layer exhibiting free surface plasmons could be used for grafting of zwitterionic molecules *via* diazonium functionality;
- Zwitterionic interface on such particles provides resistivity towards non-specific protein binding; and at the same time such interface was applied for immobilization of antibodies against prostate specific antigen (PSA) applied for selective enrichment of PSA from serum samples with subsequent electrochemical assays.

The approach presented here using hybrid magnetic particles can be easily applied for immobilization of antibodies using a highly robust surface patterning protocols *i.e.* by formation of a self-assembled monolayer with delivery of functional groups on the outer surface of magnetic particles. Hybrid magnetic particles with immobilized antibodies are applied for highly efficient and quick separation of protein of interest *i.e.* PSA from complex sample. Finally, hybrid magnetic particles with "fished-out" protein molecules could be incubated with

DOI of original article: http://dx.doi.org/10.1016/j.bios.2019.01.052
* Corresponding author at: Institute of Chemistry, Slovak Academy of Sciences, Dubravska cesta 9, Bratislava 845 38, Slovak Republic.
** Corresponding author at: Center for Advanced Materials, Qatar University, P.O. Box 2713, Doha, Qatar.
E-mail addresses: peter.kasak@qu.edu.qa (P. Kasak), jan.tkac@savba.sk (J. Tkac).

https://doi.org/10.1016/j.mex.2019.08.017

lectins to form a sandwich configuration for glycoprofiling of PSA.

ARTICLE INFO
Method name: The article contains description of synthesis of hybrid magnetic particles and their characterization using a battery of instrumental techniques
Keywords: Au nanoshells with a magnetic core, X-ray diffraction, Transmission electron microscopy, Fourier transform infrared spectroscopy, Nuclear magnetic resonance, X-ray photoelectron spectroscopy, Electrochemistry
Article history: Received 8 March 2019; Accepted 23 August 2019; Available online 11 September 2019

Specification Table

Subject Area:	*Biochemistry, Genetics and Molecular Biology*
More specific subject area:	*Synthesis and characterization of hybrid magnetic particles and betaine derivatives*
Method name:	*The article contains description of synthesis of hybrid magnetic particles and their characterization using a battery of instrumental techniques*
Name and reference of original method:	*Bertok, T., Lorencova, L., Hroncekova, S., Gajdosova, V., Jane, E., Hires, M., Kasak, P., Kaman, O., Sokol, R., Bella, V., et al. 2019 Advanced impedimetric biosensor configuration and assay protocol for glycoprofiling of a prostate oncomarker using Au nanoshells with a magnetic core. Biosens. Bioelectron.* [1]
Resource availability:	*NA*

Method details

In order to prepare hybrid magnetic particles (Au nanoshells with a magnetic core (MPs@silica@Au)) modified by zwitterionic molecules bearing diazonium functional groups, we describe in the following sections:

1. Preparation of Au nanoshells with a magnetic core (MPs@silica@Au) particles
2. Synthesis, materials, NMR and XPS spectra for zwitterionic derivatives

Hybrid magnetic particles (Au nanoshells with a magnetic core (MPs@silica@Au)) modified by zwitterionic molecules bearing diazonium functional groups were then applied for construction of impedimetric biosensor for glycoprofiling of PSA [1].

Preparation of Au nanoshells with a magnetic core (MPs@silica@Au) particles

Synthesis of Mn-Zn ferrite cores (MZF) and their fundamental properties

Solutions of manganese(II) nitrate, zinc nitrate and iron(III) nitrate slightly acidified with nitric acid and with chemically determined metal contents were employed as starting materials. Appropriate amounts were mixed in the molar ratio of Mn:Zn:Fe = 0.6:0.4:1.80 to reach the content of 5.6 mmol of metals. The resulting solution was concentrated *in vacuo* and deoxygenated, and the subsequent manipulation was carried out under an inert atmosphere. While stirring, pH was adjusted to 10.0 by adding 2 M NaOH, which led to formation of brown precipitates. The so-obtained mixture was transferred into a Berghof DAB-2 pressure vessel equipped with a 50 mL Teflon insert and a magnetic stirring bar. The mixture was treated under autogenous pressure at 180 °C for 12 h. The filling volume was 50%, and magnetic stirring was applied during the treatment. The product was washed several times with water and ethanol and was dried on air.

Powder X-ray diffraction (XRD, Bruker D8 diffractometer, CuK_{α} radiation) evidenced single phase character of the MZF product and its spinel structure with the $Fd\bar{3}m$ symmetry (for XRD pattern see

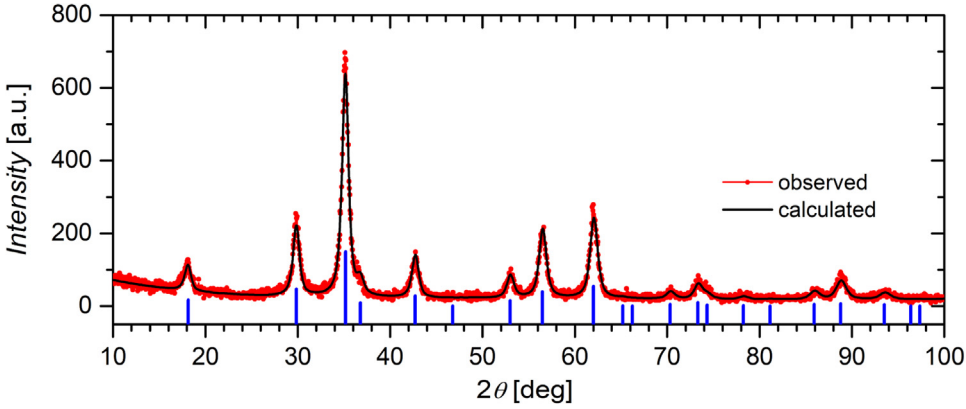

Fig. 1. XRD pattern of MZF particles. The experimental data are compared with the calculated pattern obtained by Rietveld method, the blue vertical lines indicate diffractions of the $Fd\bar{3}m$ spinel phase.

Fig. 1). The lattice parameter was refined to $a = 8.4589\,(8)$ Å by the Rietveld method. Further, the mean size of crystallites of 10 nm was evaluated based on the line broadening (the Thompson-Cox-Hastings pseudo-Voigt function was applied to resolve strain and size contributions, whereas the instrumental profile was determined by measuring a strain-free tungsten powder with crystallite size of 9.4 μm).

The actual ratio of metals in hydrothermally prepared MZF particles was analysed by X-ray fluorescence spectroscopy (XRF, Pananalytical Axios), on the basis of which the chemical composition $Mn_{0.61}Zn_{0.42}Fe_{1.97}O_4$ was determined.

Magnetic behaviour of the MZF sample was studied in DC fields by means of SQUID magnetometry (Quantum Design MPMS XL system). Specifically, the virgin curve at 5 K, hysteresis loops at 5 K and 300 K, and zero-field-cooled (ZFC) and field-cooled (FC) susceptibilities in magnetic field of $H = 1.59$ kA m^{-1},*i.e.* 20 Oe, were measured. The hysteresis loops (Fig. 2) quickly approached saturation at both the low and room temperatures, and the room-temperature magnetization reached 50.9 $Am^2\,kg^{-1}$ in a magnetic field of 1 T. The hysteresis at 5 K was characterized by coercivity of 19.9 kA m^{-1} (250 Oe), whereas the room-temperature magnetization curve was either anhysteretic due the super-paramagnetic nature of the sample or characterized by a coercivity lower than the experimental limit of the applied measurement (given by the remnant field of ≈1.2 kA m^{-1} in the superconducting winding). The ferrimagnetic arrangement of the Mn-Zn ferrite phase was characterized by the

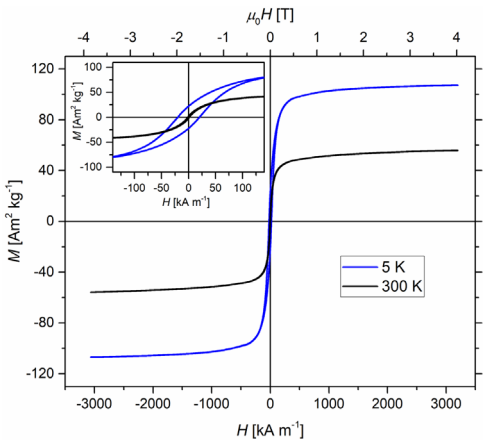

Fig. 2. Hysteresis loops of bare MZF particles at low and room temperatures. The inset shows low-field details of the loops.

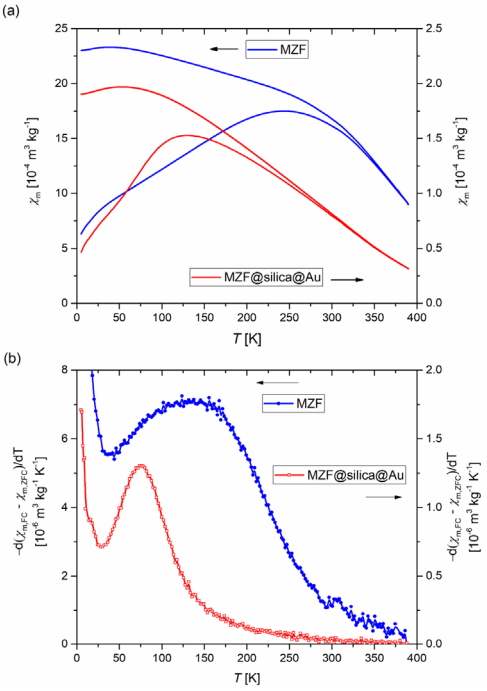

Fig. 3. ZFC-FC studies of the bare MZF sample (left axes) and the final MZF@silica@Au particles (right axes) in magnetic field of $H = 1.59$ kA m^{-1}: (a) ZFC and FC mass susceptibilities, $\chi_{m,ZFC}$ and $\chi_{m,FC}$, (b) temperature derivative of the difference of FC and ZFC susceptibilities.

moment of spontaneous ordering of 4.40 μ_B per formula unit at 5 K, which was determined by a linear extrapolation of the high-field *M-H* dependence to the zero field.

The blocking behaviour of MZF particles was analysed based on the ZFC-FC susceptibility measurements depicted in Fig. 3, in particular by considering the temperature derivative of the FC and ZFC susceptibility difference in Fig. 3**a**. The temperature derivative showed a broad peak with a maximum at ≈140 K, which corresponds to the maximum of the distribution of blocking temperatures. However, the complete onset of superparamagnetic regime within the sample of bare particles occurred at the temperature as high as ≈350 K, where the bifurcation of the ZFC/FC susceptibility was observed.

Encapsulation of ferrite cores into silica (MZF@silica)

The amount of 116 mg of MZF particles was dispersed in 10 mL of ethanol by ultrasound probe for 15 min. Then the suspension was added to 300 mL of 1.2 wt% aqueous solution of PVP K 90 in an ultrasound bath and was agitated by ultrasound overnight. The PVP-stabilized particles were separated by centrifugation and washed with 20 mL of ethanol in a single cycle. The particles were dispersed in 190 mL of ethanol in a round-bottom flask by ultrasound and mechanical stirring for 2 h. Then, 600 μL of tetraethoxysilane was added, and few minutes later 32 mL of ammonia followed. The ultrasound agitation was terminated after several minutes, and the mixture was further stirred mechanically overnight. The raw silica-coated product was separated by centrifugation and thoroughly washed with ethanol and water. The purified particles were subjected to differential centrifugation at 260 rcf for 15 min. The corresponding supernatant was collected as the final MZF@silica product, whose volume was concentrated to 20 mL.

Transmission electron microscopy (TEM, Philips CM 120 microscope) showed that the MZF@silica product was formed by small clusters of ferrite nanocrystallites covered by continuous and smooth

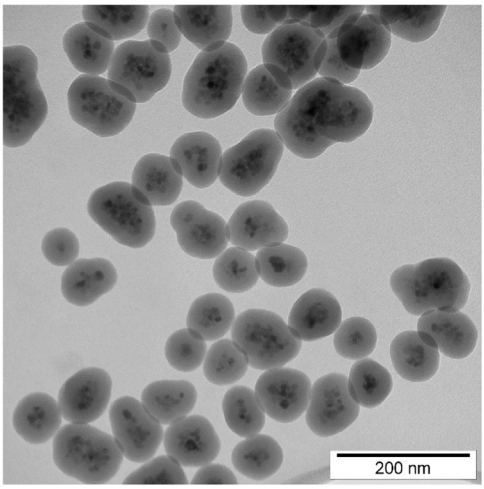

Fig. 4. Transmission electron micrograph of MZF@silica particles.

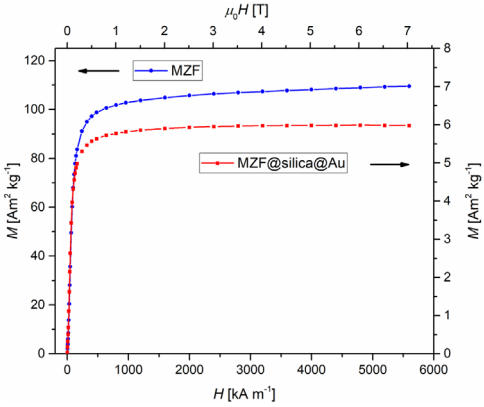

Fig. 5. Virgin magnetization curves of bare MZF nanoparticles and the final particles with gold nanoshells measured at temperature of 5 K up to magnetic field of 7 T.

silica shell. The shell exhibited quite uniform thickness with the mean value of 20 nm. For representative transmission electron micrographs see Fig. 4.

Seed-and-growth synthesis of gold nanoshells (MZF@silica@Au) and their properties

At first, fine gold nanoparticles with the size of few nanometers were synthesized according to the Duff's procedure [2]. Specifically, a solution of 0.134 μmol of tetrakis(hydroxymethyl)phosphonium chloride in 95 mL of 6.4 mM NaOH was prepared, and 4 mL of 25 mM $HAuCl_4$ solution was added while magnetic stirring was applied. The next day, the suspension was mixed with acetone to impair its colloidal stability, and the gold nanoparticles were separated by centrifugation. The particles were redispersed in pure water, and the residual acetone was evaporated *in vacuo*. The final volume of the Duff's colloid was adjusted to 100 mL.

In the meantime, MZF@silica particles were subjected to electrostatic modification by a polyelectrolyte coating deposited in three consecutive steps. In the first step, 6.66 mL of the final

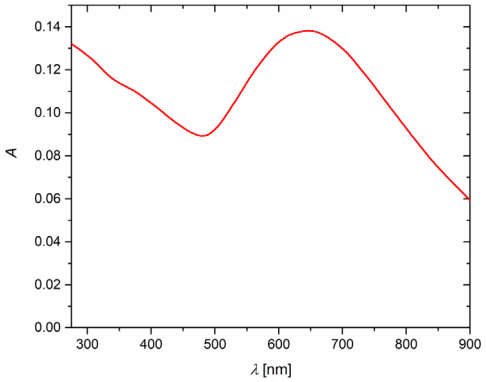

Fig. 6. UV–Vis absorption spectrum of a dilute aqueous suspension of MZF@silica@Au nanoparticles.

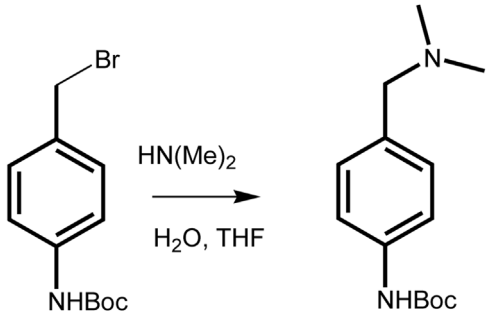

Scheme 1. Synthesis of *tert*-butyl 4-((dimethylamino)methyl)phenylcarbamate.

MZF@silica suspension was added to a solution prepared from 3 mL of water, 15 μL of 35 wt% solution of poly(diallyldimethylammonium chloride) (PDADMAC) with $M_r \approx 100{,}000$ and 4.3 mmol of NaCl. The mixture was agitated by ultrasound for 30 min, and then the particles were separated by centrifugation and redispersed in 6.66 mL of pure water. In the second step, the so-obtained particles were treated similarly with poly(sodium 4-styrenesulfonate) (PSS) with $M_r \approx 70{,}000$, supplied into the mixture as a 30 wt% solution. The third step consisted in the repeated treatment with PDADMAC. Afterwards, the modified particles were washed four times with water.

The electrostatically modified MZF@silica particles were decorated with fine gold seeds by mixing them with 100 mL of the Duff's colloid. The mixture was dispersed by ultrasound overnight, and the decorated particles were collected by centrifugation at 4,200 rcf for 30 min. During this centrifugation and during following washing cycles in water, the decorated particles sedimented, whereas the excessive free gold nanoparticles remained in supernatant and were removed from the product. The final decorated product, denoted here as MZF@silica-Au, was adjusted to the volume of 20 mL.

For the growth phase of gold nanoshell, so-called K-gold solution was prepared by dissolving 1.2 mmol of K_2CO_3 in 100 mL of 2.5 mM $HAuCl_4$ in water and ageing the resulting solution overnight. Then, 10 mL of the MZF@silica-Au suspension was mixed with 20 mL of 12 mM L-ascorbic acid in a 0.5 L round-bottom flask placed in an ultrasound bath and equipped with a mechanical stirrer. The growth of gold nanoshells was performed by continuous addition of 60 mL of the K-gold solution within 20 h *via* a syringe pump. The raw product was separated by centrifugation and washed several times with water. Finally, mild size fractionation was applied by differential centrifugation at 116 rcf

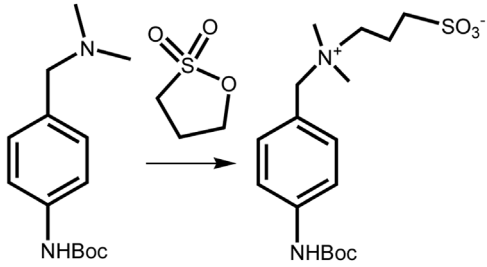

Scheme 2. Synthesis of *N*-[4-(*tert*-butyloxycarbonylamino)phenylmethyl]-*N*,*N*-dimethyl-*N*-(3-sulfopropyl) ammonium betaine.

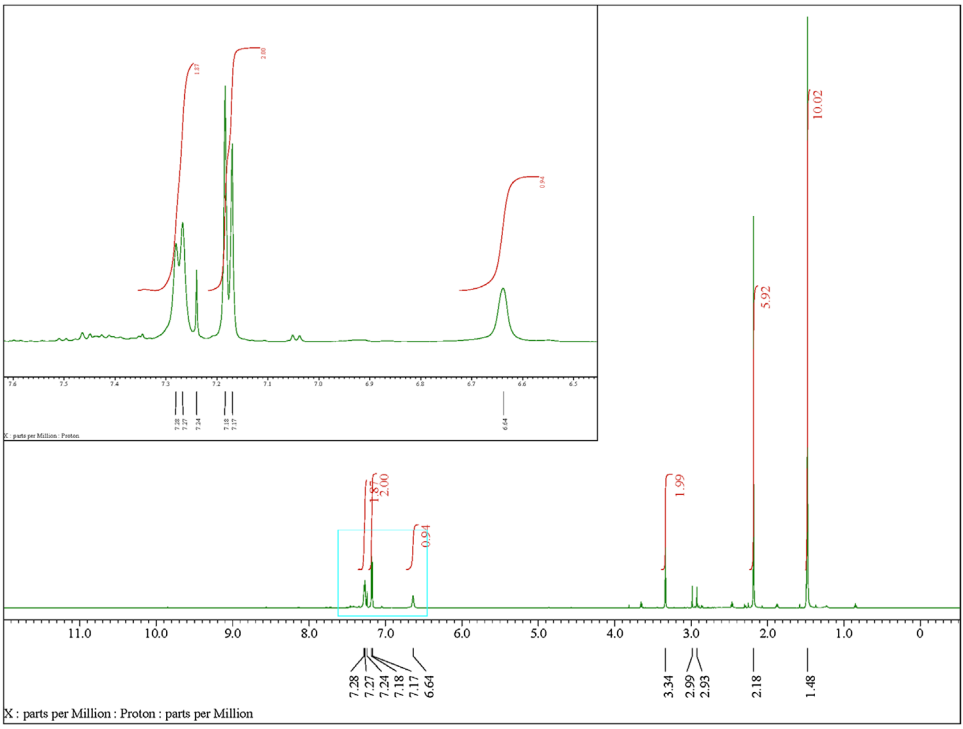

Fig. 7. ^{1}H NMR spectrum of *tert*-butyl 4-((dimethylamino)methyl)phenylcarbamate.

for 5 min to remove heavy fractions. The corresponding supernatant was collected as the final MZF@silica@Au product.

Selected magnetic measurements were carried out also on the MZF@silica@Au sample, which had been dried at 105 °C under atmospheric pressure prior to these measurements. The comparison of the low-temperature magnetization curves of the MZF nanoparticles and the final MZF@silica@Au product is shown in Fig. 5. In magnetic field of 1 T, the specific magnetization of MZF@silica@Au particles was only 5.77 $Am^2 kg^{-1}$ compared to the value of 101.8 $Am^2 kg^{-1}$ observed for MZF, which suggests that the content of the ferrite phase in the MZF@silica@Au product was roughly 6 wt%. Actually, the Mn-Zn ferrite cores in the final product were diluted by large amount of diamagnetic components, *i.e.* silica and gold, whose contribution to the total magnetic moment is almost negligible

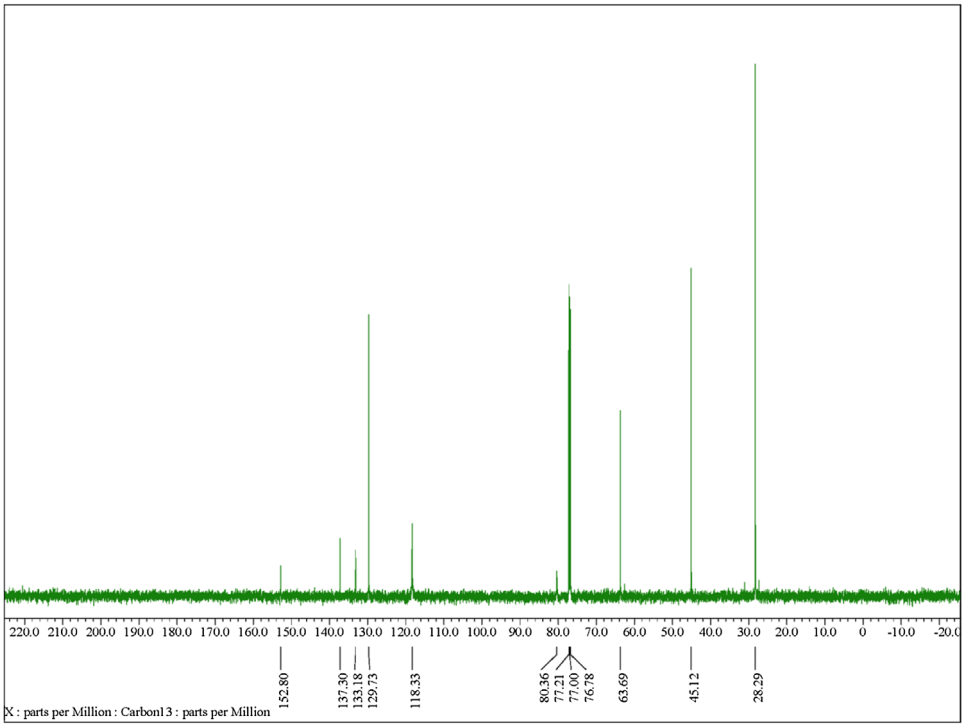

Fig. 8. ^{13}C NMR spectrum of *tert*-butyl 4-((dimethylamino)methyl)phenylcarbamate.

in low magnetic fields. Further, these components separated the small clusters of ferrite crystallites (see the micrograph in Fig. 4) by a considerable diamagnetic barrier, and thus they suppresed dipolar interactions among ferrite particles, which led to the shift of blocking events to lower temperatures (see Fig. 3). Consequently, magnetic cores of the MZF@silica@Au were completely in a superparamagnetic state at room temperature.

The UV–Vis spectrum (Shimadzu UV–1800 spectrophotometer) of an aqueous suspension of MZF@silica@Au particles was characterized by a broad absorption band with the maximum at 650 nm (see Fig. 6), which corresponds to the surface plasmon resonance of the present gold nanoshells.

Synthesis, materials, NMR and XPS spectra for zwitterionic derivatives

Synthesis of SB and CB derivatives

Zwitterionic diazonium salts were synthetized according to Scheme 2 shown in accompanied paper [1]. *Tert*-butyl 4-(bromomethyl)phenylcarbamate was let to react with dimethylamine to form dimethylamino derivative. For the sulfobetaine–based (SB) synthesis this derivative was let to react with 1,3-propane sultone and form Boc-protected SB derivative. For carboxybetaine-based (CB) derivative dimethylamino derivative reacted with ethyl bromoacetate and subsequently ethyl ester group was selectively deprotected in basic condition on ion exchange column IRA 400 to form Boc-protected CB derivative. Both zwitterionic Boc-protected derivatives were *in situ* deprotected from Boc group in acidic condition and formed diazonium salt in presence of *tert*-butyl nitrite to react with surface of electrode and by multiple cyclic voltammetry steps to obtain zwitterion-modified surface. The deprotection and activating diazonium salt were carried out in one step prior surface modification step due to limited thermal, oxygen and light stability of amino and diazonium salts precursors.

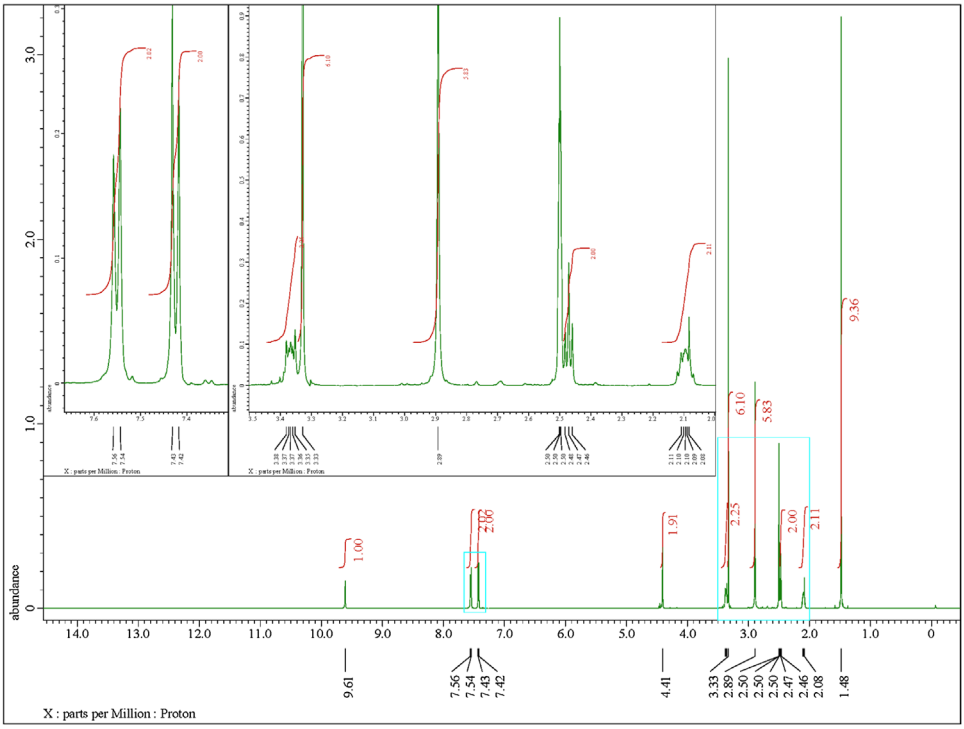

Fig. 9. ^{1}H NMR spectrum of *N*-[4-(*tert*-butyloxycarbonylamino)phenylmethyl]-*N*,*N*-dimethyl-*N*-(3-sulfopropyl) ammonium betaine.

Material

Tert-butyl 4-(bromomethyl)phenylcarbamate was prepared according to literature [3]. All other chemicals were purchased form Sigma Aldrich in high quality grade and used as received.

Synthesis of tert-butyl 4-((dimethylamino)methyl)phenylcarbamate. To solution of 250 mg bromide derivative in 4 mL THF, 3 mL of dimethylamine as 35% aq. solution was added in excess. Then solid 300 mg $NaHCO_3$ was added. The reaction mixture was stirred at ambient temperature for 24 h and evaporated. To residue, 5 mL 5% NaOH solution was added and water layer was extracted with ether 3×5 mL. Combined organic layers were dried over Na_2SO_4 and after filtration evaporated to obtain product as a white powder in 92% yield (Scheme 1). NMR spectra of *tert*-butyl 4-((dimethylamino) methyl)phenylcarbamate are shown in Figs. 7 and 8 with the following parameters extracted:

^{1}H NMR ($CDCl_3$, δ): 7.27 (2H, d, Ar-*H*), 7.20 (2H, d, Ar-*H*), 6.64 (1H, bs, N*H*), 3.33 3.61 (2H, s, ArCH_2), 2.18 (6H, s, NCH_3), 1.41 (9H, s, CCH_3).

^{13}C NMR ($CDCl_3$, δ): 152.8, 137.3, 133.2, 129.7, 118.3, 63.7, 45.1, 28.3.

Synthesis of N-[4-(tert-butyloxycarbonylamino)phenylmethyl]-N,N-dimethyl-N-(3-sulfopropyl) ammonium betaine. To 100 mg (0.4 mmol) of dimethyalamino derivate in 0.8 mL of dry acetone, 62 mg (0.55 mmol) of 1,3-propane sultone in 0.4 mL of dry acetone was added under argon atmosphere at 20 °C. The reaction mixture was stirred for 30 h. A precipitate was formed, filtrated and washed with dry diethyl ether to yield white precipitate in 69% yield (Scheme 2). NMR spectra of *N*-[4-(*tert*-butyloxycarbonylamino)phenylmethyl]-*N*,*N*-dimethyl-*N*-(3-sulfopropyl) ammonium betaine are shown in Figs. 9 and 10 with the following parameters extracted:

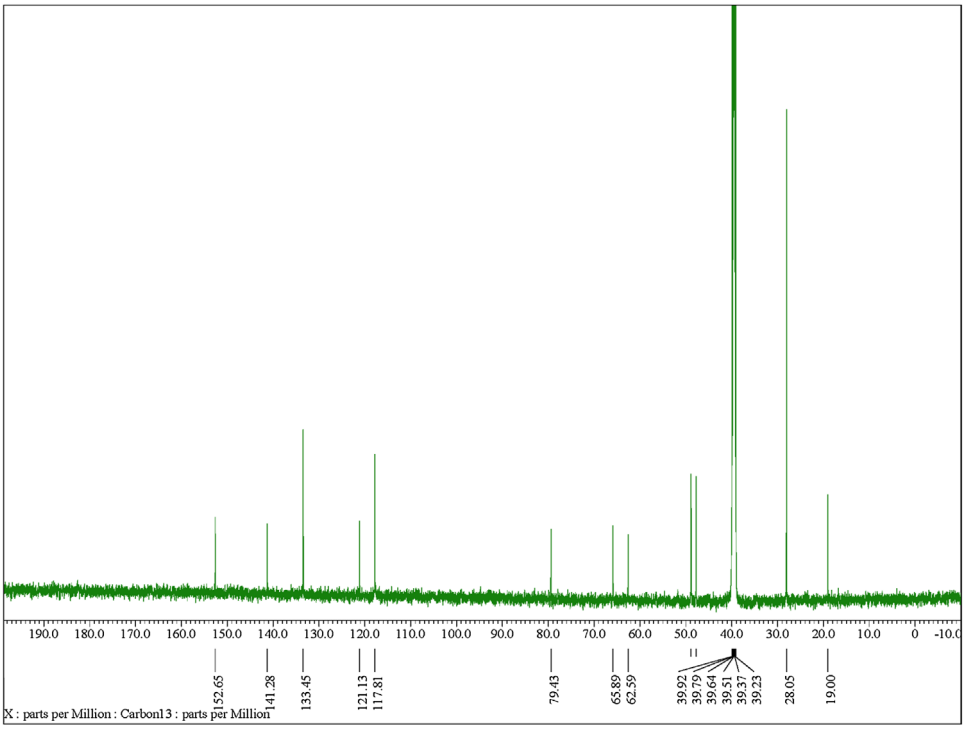

Fig. 10. ^{13}C NMR spectrum of *N*-[4-(*tert*-butyloxycarbonylamino)phenylmethyl]-*N*,*N*-dimethyl-*N*-(3-sulfopropyl) ammonium betaine.

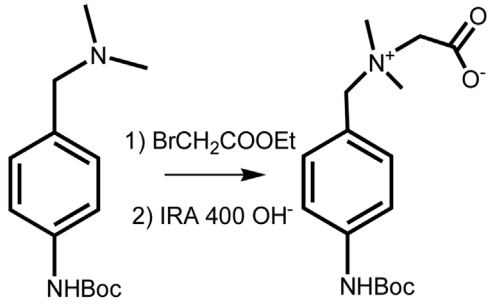

Scheme 3. Synthesis of *N*-[4-(*tert*-butyloxycarbonylamino)phenylmethyl]-*N*,*N*-dimethyl-*N*-(3-sulfopropyl) ammonium betaine.

^{1}H NMR (DMSO-d_6, δ): 9.61 (1H, s, N*H*), 7.55 (2H, d, Ar-*H*), 7.42 (2H, d, Ar-*H*), 4.40 (2H, s, Ar-CH_2), 3.37 (2H, N$^+$CH_2CH$_2$), 2.93 (6H, s, N$^+$CH_3), 2.49 (2H, d, CH_2SO$_3^-$), 2.09 (2H, m, CH$_2$CH_2CH$_2$), 1.47 (9H, s, CCH_3).

^{13}C NMR (DMSO-d_6, δ): 152.6, 141.28, 133.4, 121.1, 117.8, 79.4, 65.8, 62.7, 48.5, 47.7, 28.0.

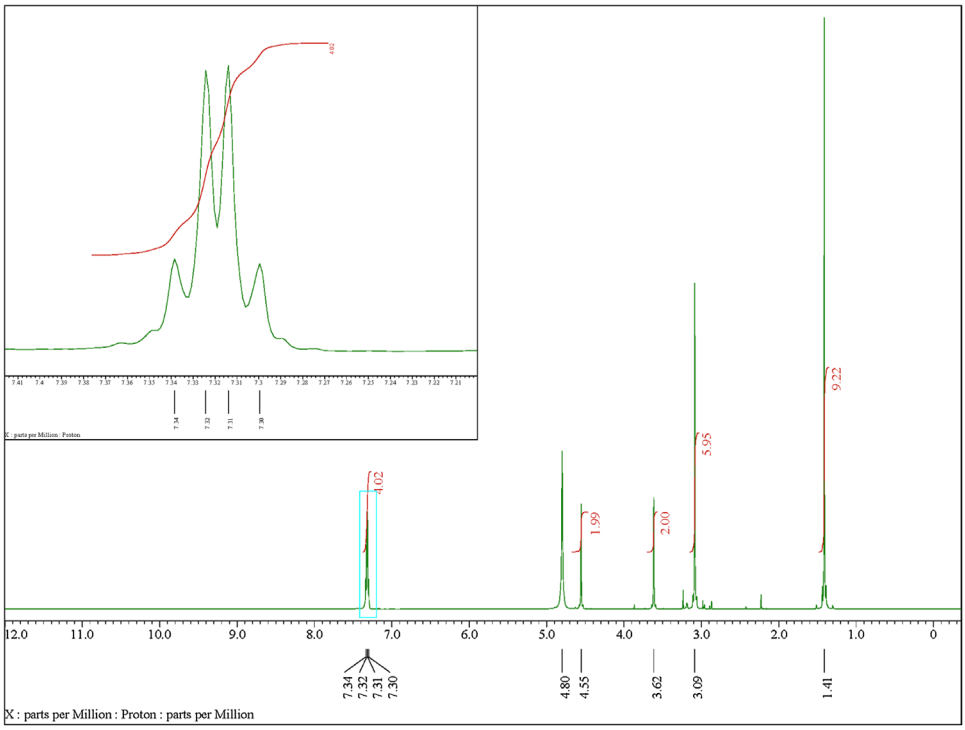

Fig. 11. ^{1}H NMR spectrum of *N*-[4-(*tert*-butyloxycarbonylamino)phenylmethyl]-*N*,*N*-dimethyl-*N*-(3-sulfopropyl) ammonium betaine.

Synthesis of N-[4-(tert-butyloxycarbonylamino)phenylmethyl]-N,N-dimethyl-N-(carboxymethyl) ammonium betaine. Ethyl bromoacetate (0.5 mmol) was added dropwise *via* syringe to solution of 100 mg dimethylamino derivative (0.4 mmol) in 1 mL of dry acetone under argon atmosphere at 20 °C. The reaction mixture was stirred for 36 h. After that the volatile substances were evaporated and the residue was dissolved in minimal volume of $CHCl_3$ and precipitated in diethyl ether. The product was dried under vacuo and yielded as hygroscopic white solid and directly dissolved in distilled water and passed throught the NaOH activated amberlite IRA 400 ion exchange column. Residual solvents were removed by rotary evaporation under reduced pressure 1 mbar to obtain a product in a form of a very hygroscopic dense oil with an overall yield of 66% in two steps (Scheme 3). NMR spectra of *N*-[4-(*tert*-butyloxycarbonylamino)phenylmethyl]-*N*,*N*-dimethyl-*N*-(3-sulfopropyl) ammonium betaine are shown in Figs. 11 and 12 with the following parameters extracted:

^{1}H NMR (D_2O, δ): 7.32 (4H, m, Ar-*H*), 4.55 (2H, s, Ar-CH_2), 3.61 (2H, s, N^+CH_2CO), 3.10 (6H, s, N^+CH_3), 1.41 (9H, s, CCH_3).

^{13}C NMR (D_2O, δ): 169.0, 154.52, 140.35, 133.5, 121.8, 119.0, 81.7, 66.3, 62.7, 50.5, 27.6.

Zwitterionic-based surface modifications. Gold electrodes surface modification was performed according to the published protocol of accompanied manuscript [1]. Briefly, 59 mM Boc-protected derivative was dissolved in deionized water (1 equivalent) and mixed with 4 equivalents of HBF_4 in acetonitrile at RT for 45 min in dark. In this step deprotection of Boc group is carried out. The acidic conditions are also required for further step of formation of diazonium salts. Thus, subsequently, reaction mixture was cooled on ice and 1.1 equivalent of *tert*-butyl nitrite was added dropwise to the

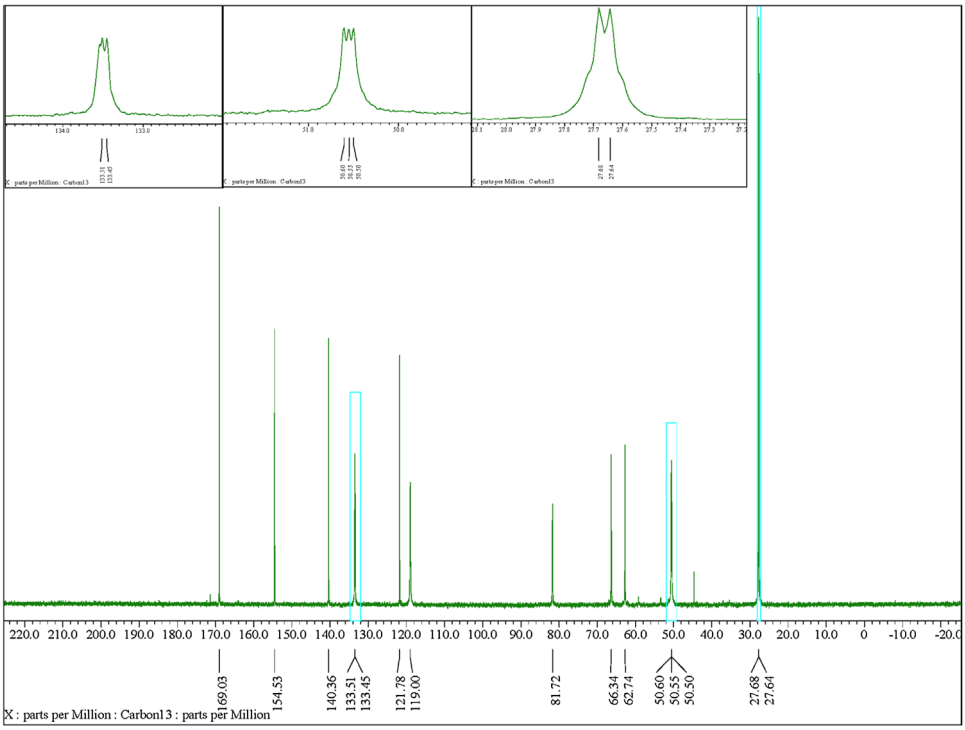

Fig. 12. ^{13}C NMR spectrum of *N*-[4-(*tert*-butyloxycarbonylamino)phenylmethyl]-*N*,*N*-dimethyl-*N*-(3-sulfopropyl) ammonium betaine.

mixture and then the solution was mixed for 2 h at room temperature. Subsequently, the solution diluted with water to obtain 2 mM solution of zwitterionic aryldiazonium salt derivative and cyclic voltammetry step from 0.0 V to −1.0 V at a scan rate of 0.25 V s^{-1} for 24 cycles was applied to obtain SAM layer on an Au electrode surface.

MP@silica@Au particles outer golden shell possesses free surface plasmons, thus the particle modification does not need to involve electrochemical grafting and proceeds spontaneously.

XPS wide survey scan of the betaine derivative immobilized on Au surface

XPS analysis was conducted to obtain information about chemical nature of the modified surface of an electrode. In a wide survey scan, all desired elements were observed (Fig. 13) and Table 1 summarizes the apparent surface chemical composition of carboxybetaine-modified surface. In high resolution spectra for N1s was observed peak at 403 eV, that corresponds to a quaternary ammonium group present in carboxybetaine structure. No additional peak is observed, what indicates neither diazonium salt nor precursor is present in the sample. Moreover, high resolution C1s spectrum showed peaks at 284, 286 and 288 eV that attributed to C—C, C—X(O,N) and C=O absorbance peak, respectively, and confirmed immobilization of carboxybetaine derivative on Au surface.

FT-IR spectra of the betaine derivative

FT-IR of SB-substrate before and after the deprotection are shown in Fig. 14.

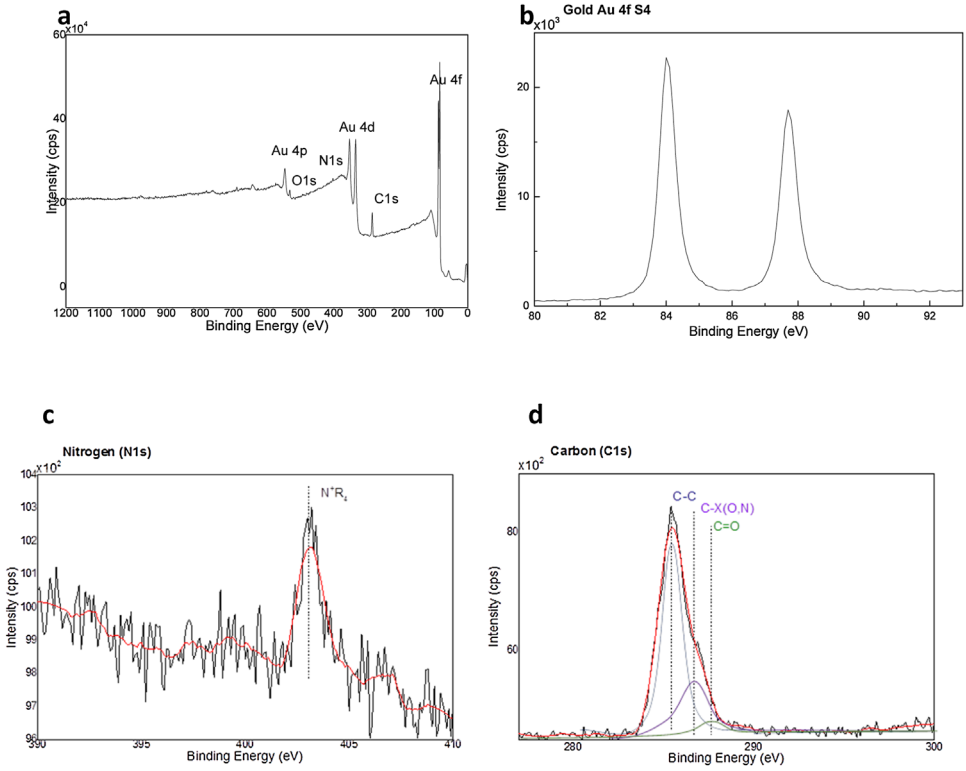

Fig. 13. XPS spectra of the final product immobilized on the gold surface; a) wide survey scan b) Au4f; c) N1s; d) C1s spectra.

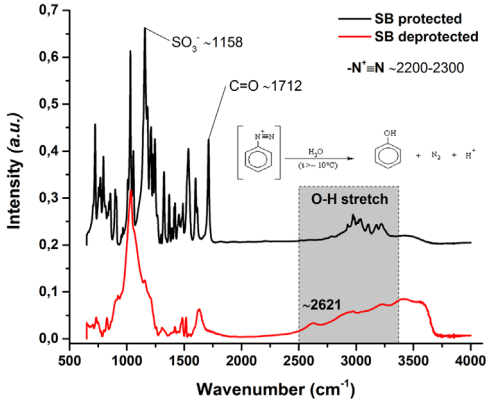

Fig. 14. FT-IR spectrum shows the appearance of a peak in the O—H stretch region (~2621 cm^{-1}), suggesting degradation of the diazonium group according to the equation in the inset. The as-prepared diazonium derivative was thus used right after preparation and was always prepared fresh *prior* to SAM layer formation.

Table 1
Surface chemical composition [at.%] from XPS analysis of carboxybetaine-modified surface.

Element	Au	C	N	O
Peak	Au4f	C1s (C—C, C—X, C=O)	N1s	O1s
Composition (at.%)	29.40	58.82 (42.44, 14.21, 2.17)	4.12	7.65

Acknowledgements

The synthesis of MP@silica@Au and some of their characterizations were supported by the Czech Science Foundation under the project 16-04340S. The financial support received from the Slovak Scientific Grant Agency VEGA2/0137/18 and 2/0090/16 from the Slovak Research and Development Agency APVV17-0300 is acknowledged. We would like to acknowledge the support from the ERC Proof of Concept grant (825586) and from the Innovative Training Network grant (No. 813120). This publication was made possible by NPRP Grant NPRP-9-219-2-105 from the Qatar National Research Fund (a member of Qatar Foundation). The statements made herein are solely the responsibility of the authors. This publication is the result of the project implementation: Centre for materials, layers and systems for applications and chemical processes under extreme conditions – Stage I, ITMS no.: 26240120007, supported by the ERDF. We would like to thank our colleague Jarmila Kulickova for the help with preparation of MP@silica@Au particles. The NMR spectra measurement was accomplished by Dr. Haw-Lih Su in the Central Laboratories Unit, Qatar University.

References

[1] T. Bertok, L. Lorencova, S. Hroncekova, V. Gajdosova, E. Jane, M. Hires, P. Kasak, O. Kaman, R. Sokol, V. Bella, A. Andicsova Eckstein, J. Mosnacek, A. Vikartovska, J. Tkac, Biosens. Bioelectron. 131 (2019) 24–29.
[2] D.G. Duff, A. Baiker, P.P. Edwards, Langmuir 9 (1993) 2301–2309.
[3] D. Antoine, D. Carine, D. Joseph, G. Roger, B. Jean-Michel, L.D. Claude, Eur. J. Org. Chem. 2014 (2014) 7699–7706.